The ER protein Ema19 facilitates the degradation of non-imported mitochondrial precursor proteins

Janina Laborenz[1], Yury S. Bykov[2], Katharina Knöringer[1], Markus Räschle[3], Sabine Filker[4], Cristina Prescianotto-Baschong[5], Anne Spang[5], Takashi Tatsuta[6], Thomas Langer[6], Zuzana Storchová[3], Maya Schuldiner[2], Johannes M. Herrmann[1*]

1, Cell Biology, University of Kaiserslautern, 67663 Kaiserslautern, Germany

2. Department of Molecular Genetics, Weizmann Institute of Science, Rehovot 7610001, Israel

3, Molecular Genetics, University of Kaiserslautern, 67663 Kaiserslautern, Germany

4, Molecular Ecology, University of Kaiserslautern, 67663 Kaiserslautern, Germany

5, Biozentrum, University of Basel, CH-4056 Basel, Switzerland

6, Max Planch Institute for Biology of Ageing, 50931 Cologne, Germany

* corresponding author:

Johannes M. Herrmann, Cell Biology, University of Kaiserslautern, Erwin-Schrödinger-Strasse 13, 67663 Kaiserslautern, Germany, +49 6312052406; hannes.herrmann@biologie.uni-kl.de, ORCID 0000-0003-2081-4506

Running title: Ema19 removes mitoproteins from the ER

Summary

For the biogenesis of mitochondria, hundreds of proteins need to be targeted from the cytosol into the various compartments of this organelle. The intramitochondrial targeting routes these proteins take to reach their respective location in the organelle are well understood. However, the early targeting processes, from cytosolic ribosomes to the membrane of the organelle, are still largely unknown. In this study, we present evidence that an integral membrane protein of the endoplasmic reticulum (ER), Ema19, plays a role in this process. Mutants lacking Ema19 show an increased stability of mitochondrial precursor proteins, indicating that Ema19 promotes the proteolytic degradation of non-productive precursors. The deletion of Ema19 improves the growth of respiration-deficient cells, suggesting that Ema19-mediated degradation can compete with productive protein import into mitochondria. Ema19 is the yeast representative of a conserved protein family. The human Ema19 homolog is known as sigma 2 receptor or TMEM97. Though its molecular function is not known, previous studies suggested a role of the sigma 2 receptor as a quality control factor in the ER, compatible with our observations about Ema19. More globally, our data provide an additional demonstration of the important role of the ER in mitochondrial protein targeting.

Introduction

Mitochondria house 800 to 1500 different proteins (Calvo *et al.*, 2016; Morgenstern *et al.*, 2017). With the exception of a very small number of mitochondrial translation products, all these proteins are synthesized on cytosolic ribosomes and need to be imported into the mitochondria. Mitochondrial targeting signals allow the specific binding of these proteins to mitochondrial surface receptors. Such receptors are part of the Translocase of the Outer Membrane, or TOM complex (Shiota *et al.*, 2015; Araiso *et al.*, 2019), which serves as the entry gate for almost all mitochondrial protein precursors. Following translocation through the

TOM complex, proteins are sorted by several additional complexes in the outer and inner membrane to their respective mitochondrial subcompartment. The mechanisms by which the mitochondrial protein import systems mediates these protein translocation reactions were analyzed in detail over the last three decades and are described in several comprehensive reviews (Chacinska *et al.*, 2009; Endo *et al.*, 2011; Callegari *et al.*, 2020; Drwesh and Rapaport, 2020; Edwards *et al.*, 2020; Mokranjac, 2020; Schneider, 2020).

The early steps of the import process which include all reactions prior to precursor binding to the TOM receptors are less well understood (Avendano-Monsalve *et al.*, 2020; Bykov *et al.*, 2020). Some precursors presumably associate with the mitochondrial surface before ribosomes complete their synthesis (Marc *et al.*, 2002; Williams *et al.*, 2014; Golani-Armon and Arava, 2016). However, in contrast to the situation for secretory proteins destined for the endoplasmic reticulum (ER), there is little evidence for a mechanistic coupling of synthesis and translocation of mitochondrial precursors. Owing to their post-translational targeting, most mitochondrial precursor proteins presumably explore the cytosol and the cytosol-exposed surface of other compartments before binding the TOM receptors (Gamerdinger *et al.*, 2015; Costa *et al.*, 2018).

Precursor proteins that accumulate in the cytosol can be highly toxic (Wang and Chen, 2015; Wrobel *et al.*, 2015) and elicit response programs to counteract these deleterious consequences (Nargund *et al.*, 2012; Weidberg and Amon, 2018; Boos *et al.*, 2019; Boos *et al.*, 2020; Song *et al.*, 2020; Zöller *et al.*, 2020). The stability of many precursor proteins in the cytosol is low thanks to surveillance of the ubiquitin/proteasome system for uninserted precursors (Bragoszewski *et al.*, 2017; Kowalski *et al.*, 2018; Paasch *et al.*, 2018; Saladi *et al.*, 2020; Shakya *et al.*, 2020). The association of mitochondrial precursors to the ER surface can retard their degradation and facilitate their productive targeting to the TOM complex by a process referred to as ER-SURF (Hansen *et al.*, 2018; Xiao *et al.*, 2020).

A recent screen in the yeast *Saccharomyces cerevisiae* (from hereon referred to as yeast) for factors that determine the cytosolic stability of mitochondrial precursor proteins identified the so-far uncharacterized protein Ema19 (Hansen *et al.*, 2018). In this study, we elucidated the relevance of Ema19 for mitochondrial biogenesis in more detail. We observe that the absence of Ema19 increases the abundance and stability of mitochondrial proteins, including those associated with the ER surface. These data suggest that Ema19 plays a role, directly or indirectly, as a quality control factor during the early, targeting, steps of the mitochondrial import process.

Results

Cells lacking Ema19 show higher levels of non-imported precursor proteins

We recently developed a genetic screen, which allows us to measure the efficiency of mitochondrial protein import on the basis of a simple growth assay (Hansen *et al.*, 2018). The assay relies on expressing a fusion between the mitochondrial inner membrane protein Oxa1 and the enzyme Ura3 (orotidine-phosphate decarboxylase) on the background of *Δura3* cells (Fig. 1A). Efficient mitochondrial import depleted cytosolic pools of the Oxa1-Ura3 fusion protein causing uracil-deficiency, whereas the cytosolic accumulation of the fusion protein (for example when its mitochondrial presequence was deleted) suppressed the uracil-dependent growth of these cells (Fig. S1A). Wild type cells expressing the Oxa1-Ura3 protein were unable to grow without uracil whereas Oxa1-Ura3 expression in cells lacking *EMA19* grew very efficiently without uracil (Fig. 1A). Thus, the absence of Ema19 apparently leads to increased cytosolic levels of the Oxa1-Ura3 fusion protein. This effect was seen very reliably in several genetic backgrounds (YPH499, W303) (Fig. S1B). This Oxa1-Ura3-mediated growth in the absence of uracil was only found in a small number of yeast mutants, including

strains with defects in the ER-associated co-chaperone Djp1 or the import component Tim50 (Hansen *et al.*, 2018).

As an independent proof for the cytosolic accumulation of Oxa1 in *Δema19* cells, we employed a fluorescence-based screen using a self-complementing split version of superfolder GFP (Pedelacq *et al.*, 2006; Smoyer *et al.*, 2016). We fused one part of GFP to the C-terminus of Oxa1 (Oxa1-GFP^{11}) and the other to the ER surface protein Sec63 (Sec63-GFP$^{1-10}$) (Fig. 1B). Using the precursor form of Oxa1 we only detected very low fluorescent levels in the WT but these were slightly increased in *Δema19* cells (Fig. 1C, S1C). Consistent with previous reports, our data indicate that under normal conditions Oxa1 precursors associate with the ER surface only very transiently (Hansen *et al.*, 2018; Shakya *et al.*, 2020; Xiao *et al.*, 2020), and that Ema19 has a role in regulating the amount or extent of this interaction. When we used an Oxa1 version that lacked its N-terminal mitochondrial targeting sequence (ΔN-Oxa1-GFP^{11}), the fluorescence signal was much higher and significantly enhanced in the *Δema19* mutant (Fig. 1D). This signal now clearly showed the characteristic pattern of an ER staining (Fig. 1E). From this we conclude that the absence of Ema19 does not lead to an initial mislocalization of mitochondrial proteins yet affects their association time with the ER or stability once they reach the ER surface (Fig. 1F).

Ema19 is highly conserved but dispensable at normal growth conditions

In an attempt to understand the role of Ema19 in mitochondrial precursor biogenesis we performed a BLAST search. Our search identified Ema19 homologs in many eukaryotic species, suggesting that Ema19 is a member of a protein family that is ubiquitously present in fungi and animals, including humans (Fig. 2A, S2). Consistently, four transmembrane domains can be predicted for these homologs indicating a conserved membrane topology.

These hydrophobic regions show many highly conserved positions and seem to be the functionally relevant segments of the Ema19 proteins (Fig. 2B, S3). N-terminal signal sequences are absent and the human Ema19 homolog, named TMEM97 or sigma 2 receptor, ends with a C-terminal KRKKK sequence that is similar to the canonical KKXX/KXKXX di-lysine ER retrieval signal found in many resident membrane proteins of the ER (Gaynor *et al.*, 1994; Ma and Goldberg, 2013). Fusing Ema19 to GFP indeed confirmed a stable ER localization of Ema19 similar to previously published data on the human protein (Bartz *et al.*, 2009; Alon *et al.*, 2017; Hansen *et al.*, 2018)(Fig. 2C). Despite the high conservation of the protein, yeast mutants lacking Ema19 did not show any obvious growth defects on fermentable (glucose, galactose) or non-fermentable (glycerol) carbon sources (Fig. 2D).

Cells lacking Ema19 show morphological changes upon respiratory growth conditions

We next used electron microscopy to visualize the ultrastructure of *Δema19* mutants (Fig. 3A, B, Fig. S4). Wild type and *Δema19* cells grown on glucose did not show any obvious differences. However, upon respiration-inducing growth conditions on glycerol we observed the accumulation of intracellular structures in the *Δema19* cells which were not observed in wild type cells. These structures were not observed by the lipid-staining reagent BODIPY 493/503 (Fig. S5). Moreover, when we performed lipidomics under the same growth conditions (growth on glycerol), we did not observe any major changes in phospholipids (Fig. 3C, D). From this we conclude that Ema19 protects cells from defects that are observed specifically when cells grow on respiratory media, thus, at conditions which induce the biogenesis of mitochondria.

The absence of Ema19 leads to increased intracellular levels of some mitochondrial proteins

Since Ema19 loss affected Oxa1 fusion protein accumulation in the cytosol we explored the effect of losing Ema19 on the levels of several mitochondrial proteins from various subcompartments (Fig. 4A). We observed, that the abundance of most tested mitochondrial proteins was unchanged. However, the levels of the IMS protein Erv1 were considerably increased by about 50% (Fig. 4B, S6A). Unfortunately, we were not able to test whether Ema19 influences the import reaction of Erv1 as in our hands, *in vitro* synthesized Erv1 was not imported into isolated mitochondria. However, we tested the import reaction of several other proteins, including Oxa1, Mrpl40, Cox19 or Cmc1, using isolated mitochondria or semi-intact cells in *in vitro* import reactions (Hansen *et al.*, 2018; Laborenz *et al.*, 2019). Wild type and *Δema19* mitochondria imported these proteins with the same efficiency (Fig. 4C, D, Fig. S6B-G). This suggests that Ema19 has no direct relevance for the protein import into mitochondria, but influences mitochondrial protein biogenesis on another step.

Ema19 interacts with many membrane proteins of the ER, of the vacuole and of mitochondria

Is Ema19 monomeric or part of a larger complex? To address this question, we made use of the Ema19-GFP strain in which we had observed the ER localization of the protein. Wild type and Ema19-GFP cells were grown on glucose and lysed with the non-ionic detergent NP40. Ema19-GFP was isolated using magnetic GFP-Trap beads and recovered proteins were identified by mass spectrometry (Fig. 5A). Ema19 was strongly enriched with the beads confirming the successful affinity purification procedure. No other proteins were similarly enriched suggesting that Ema19 is not part of a stable heterooligomeric complex. However,

many membrane proteins were pulled down with Ema19-GFP (in comparison to the wild type extracts), many of which were constituents of the ER, the vacuole and mitochondria (Fig. 5B, Table S5). The number of mitochondrial proteins that were co-purified with Ema19-GFP even further increased when the mitochondrial membrane potential had been dissipated by treatment with the uncoupler carbonylcyanid-m-chlorphenylhydrazon (CCCP) prior to cell lysis (Fig. 5C, S7). This indicates that Ema19 might particularly interact with those precursor proteins that failed to be imported into mitochondria. Interestingly, the mitochondrial proteins that were recovered with Ema19-GFP included almost exclusively transmembrane proteins such as Tom70, Mic60, Yta12, Tom40, Cox15, Ymc1, Oac1, Pic2, Tim11, Mic10, Fmp10. This suggests that Ema19 is an interactor of many cellular membrane proteins, including proteins which are no permanent residents of the ER.

Ema19 promotes the degradation of extramitochondrial precursor proteins

Ema19 might influence the stability of mitochondrial precursor proteins at a stage before their uptake into mitochondria. To test this, we used the established model substrate for an ER-bound precursor protein ΔN-Oxa1 (Hansen *et al.*, 2018). We expressed this protein from a regulatable *GAL* promoter in wild type and *Δema19* cells in galactose-containing medium. Then we transferred the cells to glucose-containing medium to switch off its expression and monitored the degradation of the ΔN-Oxa1 over time (Fig. 6A, B). In wild type cells, about two thirds of the ΔN-Oxa1 protein were degraded within one hour whereas only a minor fraction of ΔN-Oxa1 was degraded in *Δema19* cells. Thus, Ema19 apparently facilitates the recognition or degradation of this non-importable model protein.

Next, we asked whether a similar stabilizing effect can also be seen for Erv1. To this end, we expressed Erv1 with a heme agglutinin (HA) tag in wild type and *Δema19* cells and

radiolabeled newly synthesized proteins with ^{35}S methionine for ten minutes. Then, cells were washed and transferred to non-radioactive medium.

Erv1 was isolated by immunoprecipitation and its levels were visualized by autoradiography (Fig. 6C, D). Again, we observed a considerably lower turnover in *Δema19* cells than in wild type cells.

On the basis of systematic genetic screens, it was proposed that *EMA19* interacts genetically with many genes coding for subunits of the respiratory chain (Costanzo *et al.*, 2010). This observation inspired us to analyze the growth of double mutants lacking *EMA19* and genes required for respiration, such as *OXA1*, *COX23*, *QCR2* or *COA4* (Fig. 6E). None of these mutants was able to grow on the non-fermentable carbon source glycerol. However, very surprisingly, we observed that the absence of Ema19 improved growth of all of these double mutants on glucose, particularly at 37°C. Thus, the absence of Ema19 apparently suppresses some of the defects in these respiration-incompetent strains suggesting that it may allow a longer window of opportunity for precursors to enter mitochondria under limiting conditions.

Discussion

The molecular reactions by which mitochondrial proteins are recognized on the mitochondrial surface and threaded through the protein-conducting channels of the mitochondrial protein translocases were elucidated in great detail. These fascinating mechanistic insights were obtained from extremely powerful *in vitro* assays with isolated mitochondria to which radiolabeled precursor proteins were mixed. The posttranslational mode of the import reaction, the stability of mitochondrial membranes, the efficiency of the reaction for most mitochondrial proteins tested and the possibility to regulate and stage the reaction by changing the energetic conditions made this *in vitro* assay superior over other approaches.

However, unfortunately, this assay is largely blind to the initial steps that occur in between protein synthesis and precursor binding to the TOM complex under physiological *in vivo* conditions where other cellular membranes and structures are crowding the cell.

A number of recent studies reported alternative approaches to follow the import reaction which resulted in surprising observations: (1) Ribosome profiling revealed that cytosolic chaperones and the signal recognition particle play crucial roles in distinguishing mitochondrial and secretory proteins already at very early steps in their synthesis (Schibich *et al.*, 2016; Doring *et al.*, 2017; Costa *et al.*, 2018); (2) proximity labeling suggested that some mitochondrial proteins, in particular hydrophobic inner membrane proteins, explore the mitochondrial surface already during their synthesis (Jan *et al.*, 2014; Williams *et al.*, 2014; Vardi-Oknin and Arava, 2019; Wang *et al.*, 2019) and that, *in vivo*, many (if not most) mitochondrial surface proteins are in direct proximity to the ER (Hung *et al.*, 2017; Cho *et al.*, 2020); (3) systematic screens of GFP-tagged protein libraries showed that many mitochondrial proteins are prone to accumulate in non-mitochondrial locations under certain growth conditions, in particular on the ER and within the nucleus (Vitali *et al.*, 2018; Backes *et al.*, 2020; Saladi *et al.*, 2020; Shakya *et al.*, 2020; Xiao *et al.*, 2020) and, maybe even more surprising, observed non-mitochondrial residents in mitochondria (Ruan *et al.*, 2017; Bader *et al.*, 2020); and (4) genetic screens reported a very close cooperation of the mitochondrial and ER surface in protein biogenesis (Kornmann *et al.*, 2009; Papic *et al.*, 2013; Okreglak and Walter, 2014; Gamerdinger *et al.*, 2015; Wohlever *et al.*, 2017; Hansen *et al.*, 2018; Vitali *et al.*, 2018; Dederer *et al.*, 2019; Matsumoto *et al.*, 2019). Thus, *in vivo*, the surfaces of the ER and of mitochondria apparently vividly cooperate to sort proteins to the correct intracellular location.

Ema19 was identified in such a genetic screen for proteins which prevent the cytosolic accumulation of the Oxa1-Ura3 fusion protein (Hansen *et al.*, 2018). The data shown in this

study suggest that Ema19 is a protein of the ER membrane that is critical for the degradation of mitochondrial precursor proteins (Fig. 6F). It is not clear whether Ema19 interacts with these precursors directly. However, the large number of mitochondrial proteins that were co-purified with Ema19-GFP, in particular after dissipation of the mitochondrial membrane potential which blocks mitochondrial import, indicates that Ema19 serves as ER receptor for these stranded proteins. At least three pathways are known which lead to the degradation of ER-associated mitochondrial precursor proteins: (1) The components of the ER-associated degradation system as well as Cdc48 (VCP/p97 in mammals) are known to facilitate the proteasomal degradation of these proteins (Dederer *et al.*, 2019; Matsumoto *et al.*, 2019). (2) Autophagy was shown to play an important role in clearing off non-productive proteins from the ER surface (Loi *et al.*, 2019; Schäfer *et al.*, 2020). (3) Two recent studies discovered the ER protein Spf1 (P5A-ATPase in mammals) as a transmembrane helix dislocase that extracts missorted mitochondrial tail-anchored proteins from the ER membrane (McKenna *et al.*, 2020; Qin *et al.*, 2020). Interestingly, Spf1 was among the proteins that we coisolated with Ema19-GFP (see Fig. 5A) and Ema19 might support the Spf1-mediated extraction of mitochondrial precursor proteins.

Substrates of the Mia40-dependent import pathway are more slowly imported than matrix proteins and their cytosolic forms are often rather stable (Glerum *et al.*, 1996; Fischer *et al.*, 2013; Kowalski *et al.*, 2018; Habich *et al.*, 2019; Mohanraj *et al.*, 2019; Murschall *et al.*, 2020). This might explain why we found higher levels of the Mia40 substrate Erv1 (Kallergi *et al.*, 2012) but not of other mitochondrial proteins we tested. The mitochondrial import machinery and the cytosolic degradation system compete for these Mia40 substrates (Bragoszewski *et al.*, 2017; Kowalski *et al.*, 2018; Mohanraj *et al.*, 2019). Consistent with this idea, we observed that in the context of respiration-incompetent mutants, where the low membrane potential renders protein import inefficient, the deletion of Ema19 increases the

growth. Apparently, reducing the degradation of mitochondrial precursors increases the chance of these proteins to be imported.

Ema19 belongs to a protein family which is conserved among eukaryotes. The human ortholog TMEM97 or sigma 2 receptor has been implicated to play critical roles in multiple cellular dysfunctions including tumor formation, inflammation and neurodegeneration (Tesei *et al.*, 2018; Schmidt and Kruse, 2019; Zeng *et al.*, 2020) potentially caused by disturbed cholesterol homeostasis (Bartz et al., 2009).

Sigma receptors were identified as binding sites for a number of pharmaceuticals but physiological ligands are not known. Although, the anti-proliferating effect of these pharmaceuticals and their potential as anticancer drugs raised much interest, the physiological role of sigma factors is not clear. The sigma 1 receptor is a single-spanning membrane protein that forms homotrimers in the ER (Schmidt *et al.*, 2016). It is enriched at the mitochondria-associated membrane (MAM) fraction of the ER and was proposed to serve as 'membrane chaperone', though molecular details about its molecular activity are unknown (Hayashi *et al.*, 2009; Fukunaga *et al.*, 2015; Delprat *et al.*, 2020). Even less is known about the sigma 2 receptor which has no structural similarity with sigma 1 receptors but is targeted by the same pharmaceuticals. Its molecular nature was only unraveled a few years ago and found to be identical to the ER protein TMEM97 (Alon *et al.*, 2017). Several molecular processes were linked to sigma 2 receptor activity, including sterol transport, apoptosis, mitochondrial ROS production, membrane protein trafficking, and the binding and sequestration of misfolded proteins (Bartz *et al.*, 2009; Schmidt and Kruse, 2019). Due to the latter activity, the sigma receptors were also referred to as 'ER stress gatekeepers' (Tesei *et al.*, 2018). This function is also supported by our observations in this study which suggest that the yeast homolog of the sigma 2 receptor, Ema19, is critical for the removal of mitochondrial precursor proteins on the ER surface. Like TMEM97, the mitoprotein extractor of the ER, Spf1/P5A-ATPAse, was

found to influence sterol homeostasis and its molecular function was elusive until very recently (Cronin *et al.*, 2000; Sorensen *et al.*, 2015; Sorensen *et al.*, 2019). It will be exciting to use yeast as a model to elucidate the function of the Ema19/TMEM97/sigma 2 receptor protein family in more detail. More globally, our studies provide another example of the importance of ER membrane proteins in ensuring the fidelity of mitochondrial protein import.

Materials and Methods

Yeast strains and plasmids

Yeast strains used in this study are based on the wild type strains YPH499 (MATa *ura3 lys2 ade2 trp1 his3 leu2*). However, for some experiments BY4742 (MATα *his3 leu2 lys2 ura3*) or W303 (MATa *ura3 ade2 trp1 his3 leu2*) were used (see Tables in Supplemental Information). The plasmids with the superfolder splitGFP sequences were cloned by Gibson assembly (Gibson *et al.*, 2009). To generate the plasmids, the coding regions of Oxa1 (residues 1 through 402) or ΔN-Oxa1 (residues 43 through 402) were amplified from genomic DNA introducing the sequence for GFP^{11} (Smoyer *et al.*, 2016) into the downstream primer and ligated into the EcoR1 and Sma1 sites of a pYX142 vector. We had obtained the sequence for the GFP^{11} part from the information to the pRS315pr-GFP11-mCherry-PUS1 plasmid on the Addgene webpage. To generate the Sec63-GFP^{1-10} the coding region of Sec63 was amplified from genomic DNA and fused upstream of the sequence for GFP^{1-10} that was amplified from pSJ2039 into the EcoR1 and Sma1 sites of a pYX122 plasmid. pSJ2039 (pRS316-NOP1pr-GFP1-10-SCS2TM) was a gift from Sue Jaspersen.

Strains were grown in yeast complete medium (1% yeast extract, 2% peptone), containing 2% of the carbon sources galactose, glucose or glycerol as indicated. Strains containing plasmids

were grown at 30°C in minimal synthetic medium containing 0.67% yeast nitrogen base and 2% glucose or 2% lactate as carbon source.

Superfolder split-GFP assay

Cells containing either the plasmids pYX142-Oxa1-GFP[11] and pYX122-Sec63-GFP[10] or pYX142-ΔN-Oxa1-GFP[11] and pYX122-Sec63-GFP[10] were grown in selective medium containing 2% glucose to mid log phase. 3 OD_{600} were harvested, resuspended in 100 µl selective medium containing 2% glucose, transferred into a black 96 well plate and centrifuged (5 min at 30 g). The fluorescence was measured at 480 nm with a fluorescence microplate reader (Clariostar, BMG labtech).

ΔN-Oxa1 degradation assay

Yeast strains containing a pYX223-ΔN-Oxa1-HA plasmid were grown in selective media containing 2% lactate. Expression of ΔN-Oxa1-HA was induced with addition of 0.5% galactose for 4 h. The cells were then shifted to selective medium containing 2% glucose. Whole cell lysates were taken over time and visualized by Western blotting.

Preparation of semi-intact cells

The protocol for the preparation of semi-intact cells was previously described in (Laborenz *et al.*, 2019). Cells were grown in full medium containing 2% galactose at 30°C and grown to mid log phase. Cells were harvested (700 g, 7 min, RT). The pellets were resuspended in 25 ml SP1 buffer (10 mM DTT, 100 mM Tris pH unadjusted) and incubated for 10 min at 30°C. After centrifugation (5 min at 1000 g), cells were resuspended in 6 ml SP2 buffer (0.6 M

sorbitol, 1x YP, 0.2% glucose, 50 mM KPi pH 7.4, 3 mg/g wet weight zymolyase) and incubated at 30°C for 30-60 min. Spheroblast formation was monitored every 15 min. After generation of the spheroblasts, they were centrifuged and resuspended in 40 ml SP3 buffer (1x YP, 1% glucose, 0.7 M sorbitol) and again incubated for 20 min at 30°C. The samples were centrifuged (5 min at 1000 g) and washed two times with 20 ml of ice cold permeabilization buffer (20 mM Hepes pH 6.8, 150 mM KOAc, 2 mM Mg(OAc)2, 0.4 M sorbitol). The pellet was resuspended in permeabilization buffer containing 0.5 mM EGTA. Aliquots were slowly frozen over liquid nitrogen for 30 min and then stored at -80°C.

Protein import into semi-intact cells

The protocol for the import of radiolabelled proteins into semi-intact cells was previously described in (Laborenz *et al.*, 2019). The cells were thawed on ice and the OD_{600} was measured. An OD_{600} 0.5 per reaction was used. To prepare radiolabelled (^{35}S-methionine) proteins for import experiments, the TNT® Quick Coupled Transcription/Translation Kit from Promega was used. Semi-intact cells were resuspended in B88 buffer (20 mM Hepes pH 6.8, 250 mM sorbitol, 150 mM KOAc, 5 mM Mg(OAc)2) containing 2 mM ATP, 2 mM NADH, 5 mM creatine phosphate, 100 µg/ml creatine phosphatase and 1 µl per reaction radiolabelled lysate. The mixture was incubated for 10 min on ice to allow the cells to take up the lysate. The samples were then incubated at 30°C and samples were taken over time. These samples were directly added into 900 µl B88 buffer containing 50 µM CCCP to stop import and then treated with or without protease for 30 min on ice. Protein digestion was stopped by adding 2 mM PMSF. The samples were centrifuged (5 min, 4000 g, 4°C) and washes with B88 containing 2 mM PMSF. After a last centrifugation step (10 min, 25000 g, 4°C), the samples were resuspended in Laemmli containing 50 mM DTT. After boiling at 96°C for 3

min, the samples were loaded on an SDS-PAGE, the gel was blotted onto a nitrocellulose membrane and visualized by autoradiography.

Pulse-chase labelling of cells and immunoprecipitation

For *in vivo* labelling of translated proteins, cells containing pYX232-Erv1-HA were grown in selective medium without methionine, cysteine and tryptophane containing 2% galactose to mid-log phase. After washing the cells with selective medium without amino acids containing 2% galactose, cells were resuspended in the same medium. Amino acids and 1 µl per reaction radiolabelled methionine were added and incubated for 10 min at 30°C. After chasing the radiolabelled methionine with ice cold methionine and cysteine, samples were taken after different time points. To stop all reactions, the samples were centrifuged and the pellet stored on ice. Trichloracidic acid (TCA) was used for protein precipitation. The pellets were supplemented with 12% TCA and incubated at -80°C for 2 h. The frozen samples were then thawed at room temperature and centrifuged (20 min at 30,000 g). The pellet was washed with ice cold 100% acetone and again centrifuged (20 min at 30,000 g). The pellet was dried 5 min at 30°C and resuspended in lysis buffer (2.5% Triton X-100, 30 mM Tris pH 8, 100 mM NaCl). The lysate was incubated on ice for 30 min and afterwards centrifuged (60 min at 30000g). For immunoprecipitation the supernatant was added to 30 µl equilibrated sepharose A beads and 3 µl HA antibody and tumbled end-over-end overnight at 4°C. The beads were centrifuged (1 min at 2,000 g) and the supernatant kept and stored. The beads were washed twice with lysis buffer, twice with wash buffer I (2.5% Triton X-100, 30 mM Tris pH 8, 100 mM NaCl, 1 M urea) and twice with wash buffer II (30 mM Tris pH 8, 100 mM NaCl). The beads were resuspended in Laemmli buffer containing 50 mM DTT and boiled for 3 min at 96°C.

Identification of Ema19-associated proteins

For co-immunoprecipitation and mass spectrometry, cells were grown in full medium containing 2% glucose to mid-log phase. For samples in which the mitochondrial membrane potential was dissipated, 100 µM CCCP was added for one hour. 10 OD_{600} were harvested and washed with water. The supernatant was removed and the pellet resuspended in lysis buffer (10 mM Tris pH 7.5, 150 mM NaCl, 0.5 mM EDTA, 0.5% NP-40) and lysed with glass bead lysis using a FastPrep-24 5 G homogenizer (MP Biomedicals) with 3 cycles of 30 s, speed 8.0 m s–1, 120-s breaks. The lysate was centrifuged (2 min at 13000 g, 4°C). The supernatant was transferred to a precooled tube and 300 µl dilution buffer (10 mM Tris pH 7.5, 150 mM NaCl, 0.5 mM EDTA) were added. 25 µl equilibrated magnetic GFP-Trap A beads were added to the lysate and tumbled end-over-end for 1 h at 4°C.Afterwards the supernatant was discarded. The beads were then washed three times with 800 µl wash buffer I (150 mM NaCl, 50 mM Tris pH 7.5, 5% Glycerol, 0.05% NP40). After adding wash buffer I for the first time, the beads were transferred to a new tub to get rid of the detergent. Then the beads were washed with 500 µl wash buffer II (150 mM NaCl, 50 mM Tris pH 7.5, 5% Glycerol). After wash buffer II was removed completely, 50 µl elution buffer I (2 M urea, 50 mM Tris pH 7.5, 1 mM DTT, 5 ng/µl trypsin) was added to the beads for an on-bead digest and incubated for 1 h at room temperature. 15 ng/µl fresh trypsin was added for another 10 min at room temperature. Afterwards the supernatant containing the peptides was transferred to a fresh tube. 50 µl elution buffer II (2 M urea, 50 mM Tris pH 7.5, 5 mM chloroacetamide) was added for alkylating the peptides overnight in the dark at room temperature. For purification of peptides on C18 stage tips, the stage tips were washed with 100 µl methanol (5 min at 500 g), 100 µl buffer B (0.1% formic acid, 80% acetonitrile in MS grade water) and then with 100 µl buffer A (0.1% formic acid in MS grade water). To acidify the samples, they were treated with TFA to get a pH <2. The acidified peptides were then added onto the stage tips and

centrifuged (5 min at 500 g). After a last wash step with 100 µl buffer A, the peptides were eluted with 60 µl buffer B (5 min, 500 g). The samples were dried in a speed vac. Then 9 µl buffer A and 1 µl buffer A* (0.1% formic acid, 0.1% TFA in MS grade water) were added and the samples were used for mass spectrometry.

Data Availability

The mass spectrometry proteomics data have been deposited to the ProteomeXchange Consortium via the PRIDE (Perez-Riverol *et al.*, 2019) partner repository with the dataset identifier PXD022660.

Reviewer account details:

Username: reviewer_pxd022660@ebi.ac.uk

Password: Tj5NJsrr

Miscellaneous

The following methods were used as described: lipid analysis of yeast cells (Aaltonen *et al.*, 2016; Velazquez *et al.*, 2016); electron microscopy, isolation of mitochondria and import of radiolabeled proteins (Laborenz *et al.*, 2019); mass spectrometry (Backes *et al.*, 2020; Saladi *et al.*, 2020).

Acknowledgements

We thank Sabine Knaus and Lena Krämer for technical assistance, Katja Hansen for discussion and advice, and Sue Jasperson for the plasmids and protocols for the splitGFP screen. This project was funded by grants from the Deutsche Forschungsgemeinschaft (DIP MitoBalance to MS, TL and JMH and IRTG1830 to JMH) and the Landesschwerpunkt BioComp (to ZS and JMH). YSB was supported by an EMBO long-term fellowship. MS is an incumbent of the Dr. Gilbert Omenn and Martha Darling Professorial Chair in Molecular Genetics. The authors declare no competing financial interests.

Author contributions

JL, YSB and KK generated mutants, constructs, and cell fractions. JL, MS and JMH planned, performed and analyzed the data on the stability and the import of mitochondrial precursor proteins. MR and ZS identified Ema19 interactors by mass spectrometry. SF performed the phylogenetic analysis of Ema19 family members. CPB prepared the samples for electron microscopy and CPB and AS analyzed the data. TT and TL performed the lipidomics experiments. JMH analyzed the data, designed the experiments and wrote the manuscript to which also all other authors contributed.

Conflict of interest

The authors declare no conflict of interests.

References

Aaltonen, M.J., Friedman, J.R., Osman, C., Salin, B., di Rago, J.P., Nunnari, J., Langer, T., and Tatsuta, T. (2016). MICOS and phospholipid transfer by Ups2-Mdm35 organize membrane lipid synthesis in mitochondria. J Cell Biol *213*, 525-534.

Alon, A., Schmidt, H.R., Wood, M.D., Sahn, J.J., Martin, S.F., and Kruse, A.C. (2017). Identification of the gene that codes for the sigma2 receptor. Proc Natl Acad Sci U S A *114*, 7160-7165.

Araiso, Y., Tsutsumi, A., Qiu, J., Imai, K., Shiota, T., Song, J., Lindau, C., Wenz, L.S., Sakaue, H., Yunoki, K., Kawano, S., Suzuki, J., Wischnewski, M., Schutze, C., Ariyama, H., Ando, T., Becker, T., Lithgow, T., Wiedemann, N., Pfanner, N., Kikkawa, M., and Endo, T. (2019). Structure of the mitochondrial import gate reveals distinct preprotein paths. Nature *575*, 395-401.

Avendano-Monsalve, M.C., Ponce-Rojas, J.C., and Funes, S. (2020). From cytosol to mitochondria: the beginning of a protein journey. Biol Chem *401*, 645-661.

Backes, S., Bykov, Y.S., Räschle, M., Zhou, J., Lenhard, S., Krämer, L., Mühlhaus, T., Bibi, C., Jann, C., Smith, J.D., Steinmetz, L.M., Rapaport, D., Storchová, Z., Schuldiner, M., Boos, F., and Herrmann, J.M. (2020). The mitochondrial surface receptor Tom70 protects the cytosol against mitoprotein-induced stress. bioRxiv, 2020.2009.2014.296194.

Bader, G., Enkler, L., Araiso, Y., Hemmerle, M., Binko, K., Baranowska, E., De Craene, J.O., Ruer-Laventie, J., Pieters, J., Tribouillard-Tanvier, D., Senger, B., di Rago, J.P., Friant, S., Kucharczyk, R., and Becker, H.D. (2020). Assigning mitochondrial localization of dual localized proteins using a yeast Bi-Genomic Mitochondrial-Split-GFP. Elife *9*, e56649

Bartz, F., Kern, L., Erz, D., Zhu, M., Gilbert, D., Meinhof, T., Wirkner, U., Erfle, H., Muckenthaler, M., Pepperkok, R., and Runz, H. (2009). Identification of cholesterol-regulating genes by targeted RNAi screening. Cell Metab *10*, 63-75.

Boos, F., Kramer, L., Groh, C., Jung, F., Haberkant, P., Stein, F., Wollweber, F., Gackstatter, A., Zoller, E., van der Laan, M., Savitski, M.M., Benes, V., and Herrmann, J.M. (2019). Mitochondrial protein-induced stress triggers a global adaptive transcriptional programme. Nat Cell Biol *21*, 442-451.

Boos, F., Labbadia, J., and Herrmann, J.M. (2020). How the Mitoprotein-Induced Stress Response Safeguards the Cytosol: A Unified View. Trends Cell Biol *30*, 241-254.

Bragoszewski, P., Turek, M., and Chacinska, A. (2017). Control of mitochondrial biogenesis and function by the ubiquitin-proteasome system. Open Biol *7*, 170007.

Bykov, Y.S., Rapaport, D., Herrmann, J.M., and Schuldiner, M. (2020). Cytosolic Events in the Biogenesis of Mitochondrial Proteins. Trends Biochem Sci *45*, 650-667.

Callegari, S., Cruz-Zaragoza, L.D., and Rehling, P. (2020). From TOM to the TIM23 complex - handing over of a precursor. Biol Chem *401*, 709-721.

Calvo, S.E., Clauser, K.R., and Mootha, V.K. (2016). MitoCarta2.0: an updated inventory of mammalian mitochondrial proteins. Nucleic Acids Res *44*, D1251-1257.

Chacinska, A., Koehler, C.M., Milenkovic, D., Lithgow, T., and Pfanner, N. (2009). Importing mitochondrial proteins: machineries and mechanisms. Cell *138*, 628-644.

Cho, K.F., Branon, T.C., Rajeev, S., Svinkina, T., Udeshi, N.D., Thoudam, T., Kwak, C., Rhee, H.W., Lee, I.K., Carr, S.A., and Ting, A.Y. (2020). Split-TurboID enables contact-dependent proximity labeling in cells. Proc Natl Acad Sci U S A *117*, 12143-12154.

Costa, E.A., Subramanian, K., Nunnari, J., and Weissman, J.S. (2018). Defining the physiological role of SRP in protein-targeting efficiency and specificity. Science *359*, 689-692.

Costanzo, M., Baryshnikova, A., Bellay, J., Kim, Y., Spear, E.D., Sevier, C.S., Ding, H., Koh, J.L., Toufighi, K., Mostafavi, S., Prinz, J., St Onge, R.P., VanderSluis, B., Makhnevych, T., Vizeacoumar, F.J., Alizadeh, S., Bahr, S., Brost, R.L., Chen, Y., Cokol, M., Deshpande, R., Li, Z., Lin, Z.Y., Liang, W., Marback, M., Paw, J., San Luis, B.J., Shuteriqi, E., Tong, A.H., van Dyk, N., Wallace, I.M., Whitney, J.A., Weirauch, M.T., Zhong, G., Zhu, H., Houry, W.A., Brudno, M., Ragibizadeh, S., Papp, B., Pal, C., Roth, F.P., Giaever, G., Nislow, C., Troyanskaya, O.G., Bussey,

H., Bader, G.D., Gingras, A.C., Morris, Q.D., Kim, P.M., Kaiser, C.A., Myers, C.L., Andrews, B.J., and Boone, C. (2010). The genetic landscape of a cell. Science *327*, 425-431.
Cronin, S.R., Khoury, A., Ferry, D.K., and Hampton, R.Y. (2000). Regulation of HMG-CoA reductase degradation requires the P-type ATPase Cod1p/Spf1p. J Cell Biol *148*, 915-924.
Dederer, V., Khmelinskii, A., Huhn, A.G., Okreglak, V., Knop, M., and Lemberg, M.K. (2019). Cooperation of mitochondrial and ER factors in quality control of tail-anchored proteins. Elife *8*.
Delprat, B., Crouzier, L., Su, T.P., and Maurice, T. (2020). At the Crossing of ER Stress and MAMs: A Key Role of Sigma-1 Receptor? Adv Exp Med Biol *1131*, 699-718.
Doring, K., Ahmed, N., Riemer, T., Suresh, H.G., Vainshtein, Y., Habich, M., Riemer, J., Mayer, M.P., O'Brien, E.P., Kramer, G., and Bukau, B. (2017). Profiling Ssb-Nascent Chain Interactions Reveals Principles of Hsp70-Assisted Folding. Cell *170*, 298-311 e220.
Drwesh, L., and Rapaport, D. (2020). Biogenesis pathways of alpha-helical mitochondrial outer membrane proteins. Biol Chem *401*, 677-686.
Edwards, R., Gerlich, S., and Tokatlidis, K. (2020). The biogenesis of mitochondrial intermembrane space proteins. Biol Chem *401*, 737-747.
Endo, T., Yamano, K., and Kawano, S. (2011). Structural insight into the mitochondrial protein import system. Biochim Biophys Acta *1808*, 955-970.
Fischer, M., Horn, S., Belkacemi, A., Kojer, K., Petrungaro, C., Habich, M., Ali, M., Kuttner, V., Bien, M., Kauff, F., Dengjel, J., Herrmann, J.M., and Riemer, J. (2013). Protein import and oxidative folding in the mitochondrial intermembrane space of intact mammalian cells. Mol Biol Cell *24*, 2160-2170.
Fukunaga, K., Shinoda, Y., and Tagashira, H. (2015). The role of SIGMAR1 gene mutation and mitochondrial dysfunction in amyotrophic lateral sclerosis. J Pharmacol Sci *127*, 36-41.
Gamerdinger, M., Hanebuth, M.A., Frickey, T., and Deuerling, E. (2015). The principle of antagonism ensures protein targeting specificity at the endoplasmic reticulum. Science *348*, 201-207.
Gaynor, E.C., te Heesen, S., Graham, T.R., Aebi, M., and Emr, S.D. (1994). Signal-mediated retrieval of a membrane protein from the Golgi to the ER in yeast. J Cell Biol *127*, 653-665.
Gibson, D.G., Young, L., Chuang, R.Y., Venter, J.C., Hutchison, C.A., 3rd, and Smith, H.O. (2009). Enzymatic assembly of DNA molecules up to several hundred kilobases. Nat Methods *6*, 343-345.
Glerum, D.M., Shtanko, A., and Tzagoloff, A. (1996). Characterization of *COX17*, a yeast gene involved in copper metabolism and assembly of cytochrome oxidase. J. Biol. Chem. *271*, 14504-14509.
Golani-Armon, A., and Arava, Y. (2016). Localization of Nuclear-Encoded mRNAs to Mitochondria Outer Surface. Biochemistry (Mosc) *81*, 1038-1043.
Habich, M., Salscheider, S.L., Murschall, L.M., Hoehne, M.N., Fischer, M., Schorn, F., Petrungaro, C., Ali, M., Erdogan, A.J., Abou-Eid, S., Kashkar, H., Dengjel, J., and Riemer, J. (2019). Vectorial Import via a Metastable Disulfide-Linked Complex Allows for a Quality Control Step and Import by the Mitochondrial Disulfide Relay. Cell Rep *26*, 759-774 e755.
Hansen, K.G., Aviram, N., Laborenz, J., Bibi, C., Meyer, M., Spang, A., Schuldiner, M., and Herrmann, J.M. (2018). An ER surface retrieval pathway safeguards the import of mitochondrial membrane proteins in yeast. Science *361*, 1118-1122.
Hayashi, T., Rizzuto, R., Hajnoczky, G., and Su, T.P. (2009). MAM: more than just a housekeeper. Trends Cell Biol *19*, 81-88.
Hofmann, K., and Stoffel, W. (1993). TMbase - A database of membrane spanning proteins segments. Biol. Chem. *374*, 166.
Hung, V., Lam, S.S., Udeshi, N.D., Svinkina, T., Guzman, G., Mootha, V.K., Carr, S.A., and Ting, A.Y. (2017). Proteomic mapping of cytosol-facing outer mitochondrial and ER membranes in living human cells by proximity biotinylation. Elife *6*, e24463.
Jan, C.H., Williams, C.C., and Weissman, J.S. (2014). Principles of ER cotranslational translocation revealed by proximity-specific ribosome profiling. Science *346*, 1257521.
Kallergi, E., Andreadaki, M., Kritsiligkou, P., Katrakili, N., Pozidis, C., Tokatlidis, K., Banci, L., Bertini, I., Cefaro, C., Ciofi-Baffoni, S., Gajda, K., and Peruzzini, R. (2012). Targeting and maturation of Erv1/ALR in the mitochondrial intermembrane space. ACS Chem Biol *7*, 707-714.
Kornmann, B., Currie, E., Collins, S.R., Schuldiner, M., Nunnari, J., Weissman, J.S., and Walter, P. (2009). An ER-mitochondria tethering complex revealed by a synthetic biology screen. Science *325*, 477-481.

Kowalski, L., Bragoszewski, P., Khmelinskii, A., Glow, E., Knop, M., and Chacinska, A. (2018). Determinants of the cytosolic turnover of mitochondrial intermembrane space proteins. BMC Biol *16*, 66.

Laborenz, J., Hansen, K., Prescianotto-Baschong, C., Spang, A., and Herrmann, J.M. (2019). In vitro import experiments with semi-intact cells suggest a role of the Sec61 paralog Ssh1 in mitochondrial biogenesis. Biol Chem *400*, 1229-1240.

Liao, Y., Wang, J., Jaehnig, E.J., Shi, Z., and Zhang, B. (2019). WebGestalt 2019: gene set analysis toolkit with revamped UIs and APIs. Nucleic Acids Res *47*, W199-W205.

Loi, M., Raimondi, A., Morone, D., and Molinari, M. (2019). ESCRT-III-driven piecemeal micro-ER-phagy remodels the ER during recovery from ER stress. Nat Commun *10*, 5058.

Ma, W., and Goldberg, J. (2013). Rules for the recognition of dilysine retrieval motifs by coatomer. EMBO J *32*, 926-937.

Marc, P., Margeot, A., Devaux, F., Blugeon, C., Corral-Debrinski, M., and Jacq, C. (2002). Genome-wide analysis of mRNAs targeted to yeast mitochondria. EMBO Rep. *3*, 159-164.

Matsumoto, S., Nakatsukasa, K., Kakuta, C., Tamura, Y., Esaki, M., and Endo, T. (2019). Msp1 Clears Mistargeted Proteins by Facilitating Their Transfer from Mitochondria to the ER. Mol Cell *76*, 191-205.

McKenna, M.J., Sim, S.I., Ordureau, A., Wei, L., Harper, J.W., Shao, S., and Park, E. (2020). The endoplasmic reticulum P5A-ATPase is a transmembrane helix dislocase. Science *369*, eabc5809.

Mohanraj, K., Wasilewski, M., Beninca, C., Cysewski, D., Poznanski, J., Sakowska, P., Bugajska, Z., Deckers, M., Dennerlein, S., Fernandez-Vizarra, E., Rehling, P., Dadlez, M., Zeviani, M., and Chacinska, A. (2019). Inhibition of proteasome rescues a pathogenic variant of respiratory chain assembly factor COA7. EMBO Mol Med *11*, e9561.

Mokranjac, D. (2020). How to get to the other side of the mitochondrial inner membrane - the protein import motor. Biol Chem *401*, 723-736.

Morgenstern, M., Stiller, S.B., Lubbert, P., Peikert, C.D., Dannenmaier, S., Drepper, F., Weill, U., Hoss, P., Feuerstein, R., Gebert, M., Bohnert, M., van der Laan, M., Schuldiner, M., Schutze, C., Oeljeklaus, S., Pfanner, N., Wiedemann, N., and Warscheid, B. (2017). Definition of a High-Confidence Mitochondrial Proteome at Quantitative Scale. Cell Rep *19*, 2836-2852.

Murschall, L.M., Gerhards, A., MacVicar, T., Peker, E., Hasberg, L., Wawra, S., Langer, T., and Riemer, J. (2020). The C-terminal region of the oxidoreductase MIA40 stabilizes its cytosolic precursor during mitochondrial import. BMC Biol *18*, 96.

Nargund, A.M., Pellegrino, M.W., Fiorese, C.J., Baker, B.M., and Haynes, C.M. (2012). Mitochondrial import efficiency of ATFS-1 regulates mitochondrial UPR activation. Science *337*, 587-590.

Okreglak, V., and Walter, P. (2014). The conserved AAA-ATPase Msp1 confers organelle specificity to tail-anchored proteins. Proc Natl Acad Sci U S A *111*, 8019-8024.

Paasch, F., den Brave, F., Psakhye, I., Pfander, B., and Jentsch, S. (2018). Failed mitochondrial import and impaired proteostasis trigger SUMOylation of mitochondrial proteins. J Biol Chem *293*, 599-609.

Papic, D., Elbaz-Alon, Y., Koerdt, S.N., Leopold, K., Worm, D., Jung, M., Schuldiner, M., and Rapaport, D. (2013). The role of Djp1 in import of the mitochondrial protein Mim1 demonstrates specificity between a cochaperone and its substrate protein. Mol Cell Biol *33*, 4083-4094.

Pedelacq, J.D., Cabantous, S., Tran, T., Terwilliger, T.C., and Waldo, G.S. (2006). Engineering and characterization of a superfolder green fluorescent protein. Nat Biotechnol *24*, 79-88.

Perez-Riverol, Y., Csordas, A., Bai, J., Bernal-Llinares, M., Hewapathirana, S., Kundu, D.J., Inuganti, A., Griss, J., Mayer, G., Eisenacher, M., Perez, E., Uszkoreit, J., Pfeuffer, J., Sachsenberg, T., Yilmaz, S., Tiwary, S., Cox, J., Audain, E., Walzer, M., Jarnuczak, A.F., Ternent, T., Brazma, A., and Vizcaino, J.A. (2019). The PRIDE database and related tools and resources in 2019: improving support for quantification data. Nucleic Acids Res *47*, D442-D450.

Prescianotto-Baschong, C., and Riezman, H. (2002). Ordering of compartments in the yeast endocytic pathway. Traffic *3*, 37-49.

Qin, Q., Zhao, T., Zou, W., Shen, K., and Wang, X. (2020). An Endoplasmic Reticulum ATPase Safeguards Endoplasmic Reticulum Identity by Removing Ectopically Localized Mitochondrial Proteins. Cell Rep *33*, 108363.

Ruan, L., Zhou, C., Jin, E., Kucharavy, A., Zhang, Y., Wen, Z., Florens, L., and Li, R. (2017). Cytosolic proteostasis through importing of misfolded proteins into mitochondria. Nature *543*, 443-446.

Saladi, S., Boos, F., Poglitsch, M., Meyer, H., Sommer, F., Muhlhaus, T., Schroda, M., Schuldiner, M., Madeo, F., and Herrmann, J.M. (2020). The NADH Dehydrogenase Nde1 Executes Cell Death after Integrating Signals from Metabolism and Proteostasis on the Mitochondrial Surface. Mol Cell *77*, 189-202 e186.

Schäfer, J.A., Schessner, J.P., Bircham, P.W., Tsuji, T., Funaya, C., Pajonk, O., Schaeff, K., Ruffini, G., Papagiannidis, D., Knop, M., Fujimoto, T., and Schuck, S. (2020). ESCRT machinery mediates selective microautophagy of endoplasmic reticulum in yeast. EMBO J *39*, e102586.

Schibich, D., Gloge, F., Pohner, I., Bjorkholm, P., Wade, R.C., von Heijne, G., Bukau, B., and Kramer, G. (2016). Global profiling of SRP interaction with nascent polypeptides. Nature *536*, 219-223.

Schmidt, H.R., and Kruse, A.C. (2019). The Molecular Function of sigma Receptors: Past, Present, and Future. Trends Pharmacol Sci *40*, 636-654.

Schmidt, H.R., Zheng, S., Gurpinar, E., Koehl, A., Manglik, A., and Kruse, A.C. (2016). Crystal structure of the human sigma1 receptor. Nature *532*, 527-530.

Schneider, A. (2020). Evolution of mitochondrial protein import - lessons from trypanosomes. Biol Chem *401*, 663-676.

Shakya, V.P.S., Barbeau, W.A., Xiao, T., Knutson, C.S., and Hughes, A.L. (2020). The nucleus is a quality control center for non-imported mitochondrial proteins. bioRxiv, 2020.2006.2026.173781.

Shiota, T., Imai, K., Qiu, J., Hewitt, V.L., Tan, K., Shen, H.H., Sakiyama, N., Fukasawa, Y., Hayat, S., Kamiya, M., Elofsson, A., Tomii, K., Horton, P., Wiedemann, N., Pfanner, N., Lithgow, T., and Endo, T. (2015). Molecular architecture of the active mitochondrial protein gate. Science *349*, 1544-1548.

Smoyer, C.J., Katta, S.S., Gardner, J.M., Stoltz, L., McCroskey, S., Bradford, W.D., McClain, M., Smith, S.E., Slaughter, B.D., Unruh, J.R., and Jaspersen, S.L. (2016). Analysis of membrane proteins localizing to the inner nuclear envelope in living cells. J Cell Biol *215*, 575-590.

Song, J., Herrmann, J.M., and Becker, T. (2020). Quality control of the mitochondrial proteome. Nat Rev Mol Cell Biol.

Sorensen, D.M., Holen, H.W., Holemans, T., Vangheluwe, P., and Palmgren, M.G. (2015). Towards defining the substrate of orphan P5A-ATPases. Biochim Biophys Acta *1850*, 524-535.

Sorensen, D.M., Holen, H.W., Pedersen, J.T., Martens, H.J., Silvestro, D., Stanchev, L.D., Costa, S.R., Gunther Pomorski, T., Lopez-Marques, R.L., and Palmgren, M. (2019). The P5A ATPase Spf1p is stimulated by phosphatidylinositol 4-phosphate and influences cellular sterol homeostasis. Mol Biol Cell *30*, 1069-1084.

Tesei, A., Cortesi, M., Zamagni, A., Arienti, C., Pignatta, S., Zanoni, M., Paolillo, M., Curti, D., Rui, M., Rossi, D., and Collina, S. (2018). Sigma Receptors as Endoplasmic Reticulum Stress "Gatekeepers" and their Modulators as Emerging New Weapons in the Fight Against Cancer. Front Pharmacol *9*, 711.

Vardi-Oknin, D., and Arava, Y. (2019). Characterization of Factors Involved in Localized Translation Near Mitochondria by Ribosome-Proximity Labeling. Front Cell Dev Biol *7*, 305.

Velazquez, A.P., Tatsuta, T., Ghillebert, R., Drescher, I., and Graef, M. (2016). Lipid droplet-mediated ER homeostasis regulates autophagy and cell survival during starvation. J Cell Biol *212*, 621-631.

Vitali, D.G., Sinzel, M., Bulthuis, E.P., Kolb, A., Zabel, S., Mehlhorn, D.G., Figueiredo Costa, B., Farkas, A., Clancy, A., Schuldiner, M., Grefen, C., Schwappach, B., Borgese, N., and Rapaport, D. (2018). The GET pathway can increase the risk of mitochondrial outer membrane proteins to be mistargeted to the ER. J Cell Sci *131*.

Wang, P., Tang, W., Li, Z., Zou, Z., Zhou, Y., Li, R., Xiong, T., Wang, J., and Zou, P. (2019). Mapping spatial transcriptome with light-activated proximity-dependent RNA labeling. Nat Chem Biol *15*, 1110-1119.

Wang, X., and Chen, X.J. (2015). A cytosolic network suppressing mitochondria-mediated proteostatic stress and cell death. Nature *524*, 481-484.

Weidberg, H., and Amon, A. (2018). MitoCPR-A surveillance pathway that protects mitochondria in response to protein import stress. Science *360*, eaan4146.

Williams, C.C., Jan, C.H., and Weissman, J.S. (2014). Targeting and plasticity of mitochondrial proteins revealed by proximity-specific ribosome profiling. Science *346*, 748-751.
Wohlever, M.L., Mateja, A., McGilvray, P.T., Day, K.J., and Keenan, R.J. (2017). Msp1 Is a Membrane Protein Dislocase for Tail-Anchored Proteins. Mol Cell *67*, 194-202 e196.
Wrobel, L., Topf, U., Bragoszewski, P., Wiese, S., Sztolsztener, M.E., Oeljeklaus, S., Varabyova, A., Lirski, M., Chroscicki, P., Mroczek, S., Januszewicz, E., Dziembowski, A., Koblowska, M., Warscheid, B., and Chacinska, A. (2015). Mistargeted mitochondrial proteins activate a proteostatic response in the cytosol. Nature *524*, 485-488.
Xiao, T., Shakya, V.P.S., and Hughes, A.L. (2020). The GET pathway safeguards against non-imported mitochondrial protein stress. bioRxiv, 2020.2006.2026.173831.
Zeng, C., Riad, A., and Mach, R.H. (2020). The Biological Function of Sigma-2 Receptor/TMEM97 and Its Utility in PET Imaging Studies in Cancer. Cancers (Basel) *12*.
Zöller, E., Laborenz, J., Kramer, L., Boos, F., Raschle, M., Alexander, R.T., and Herrmann, J.M. (2020). The intermembrane space protein Mix23 is a novel stress-induced mitochondrial import factor. J Biol Chem *295*, 14686-14697.

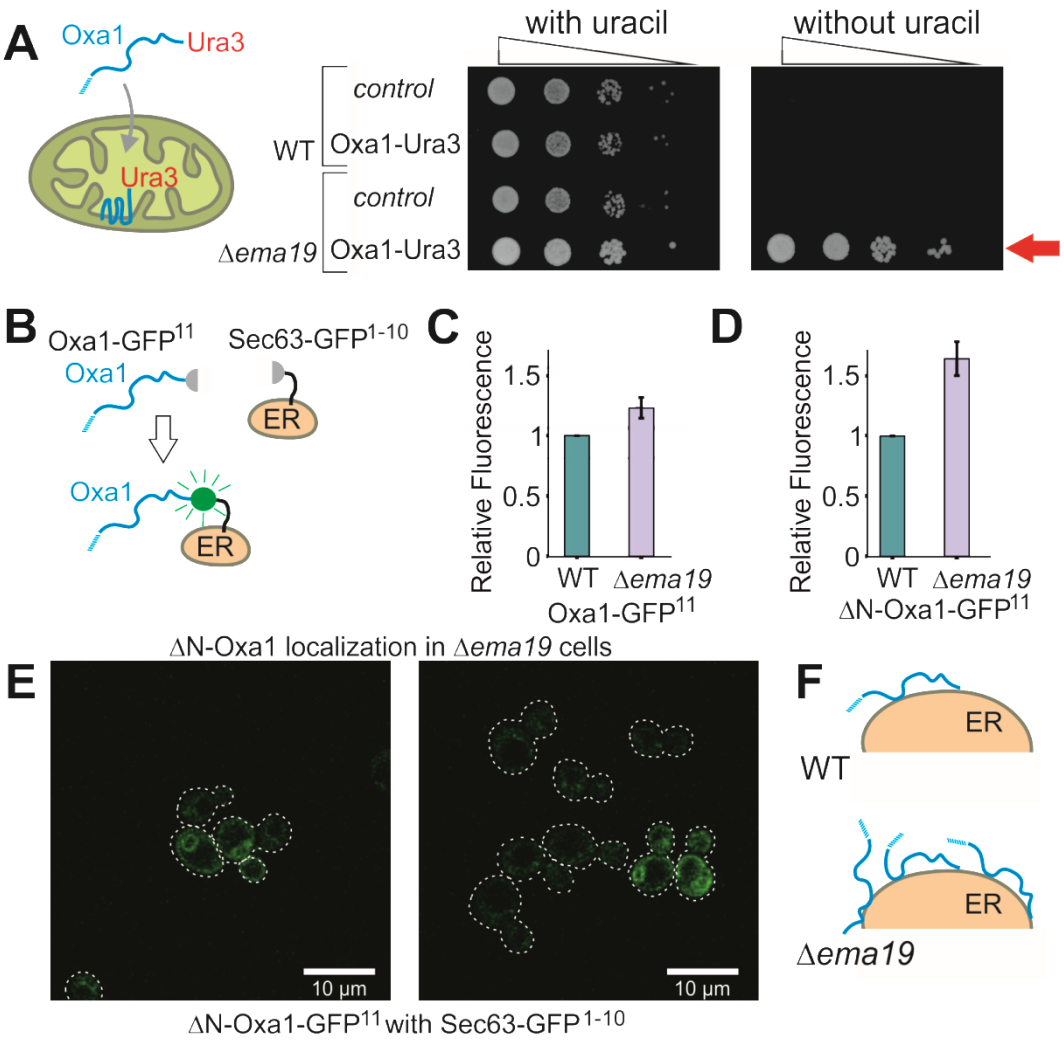

Figure legends

Figure 1. Deletion of Ema19 leads to increased levels of non-imported mitochondrial precursor proteins. A. A schematic representation of the Oxa1-Ura3 reporter assay is shown on the left. Wild type (WT) and *Δema19* cells were transformed with empty (*control*) or Oxa1-Ura3 expression plasmids and grown on uracil-containing medium to mid-log phase. Serial tenfold deletions were dropped onto glucose plates which contained or lacked uracil. The arrow depicts the efficient uracil-independent growth induced by Oxa1-Ura3 in *Δema19* cells. **B.** Schematic representation of the split-GFP assay. **C, D.** Wild type and Δ*ema19* cells expressing Sec63-GFP$^{1-10}$ and either Oxa1-GFP^{11} or ΔN-Oxa1-GFP^{11} were grown to mid-log phase before GFP-mediated fluorescence was measured. Values show mean and standard deviation values from three measurements. **E.** Microscopy pictures from the cells containing the analyzed in D. Note that the GFP signal shows the characteristic perinuclear and cortical pattern of ER proteins in yeast cells. **F.** Model for the accumulation of extra-mitochondrial precursors in *Δema19* cells.

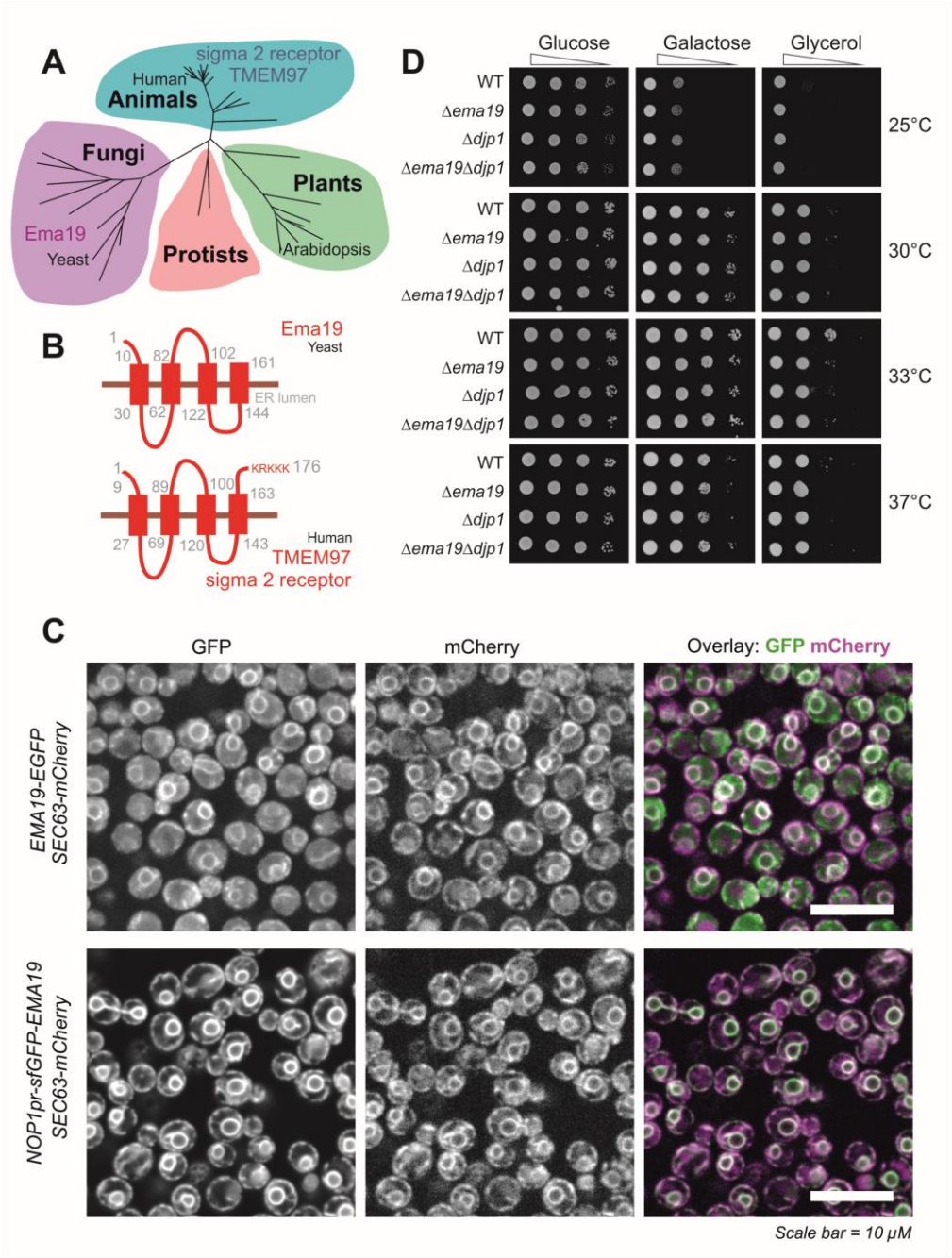

Figure 2. Ema19 belongs to a conserved family of ER proteins. A. Phylogenetic analysis of members of the Ema19/TMEM97 family (see Fig. S2 for sequence details). **B.** A model for the orientation of the Ema19 and TMEM97 is shown on the right. Transmembrane domains were predicted using TMpred (Hofmann and Stoffel, 1993). **C.** Cells expressing 'Ema19-EGFP and sfGFP-Ema19 were analyzed by fluorescence microscopy. Sec63-mCherry served as ER marker. The intense perinuclear staining of the GFP signals indicate the localization of Ema19 in perinuclear ER membranes. **D.** The respective strains were grown in galactose medium and dropped on plates containing different carbon sources and grown at the indicated temperatures.

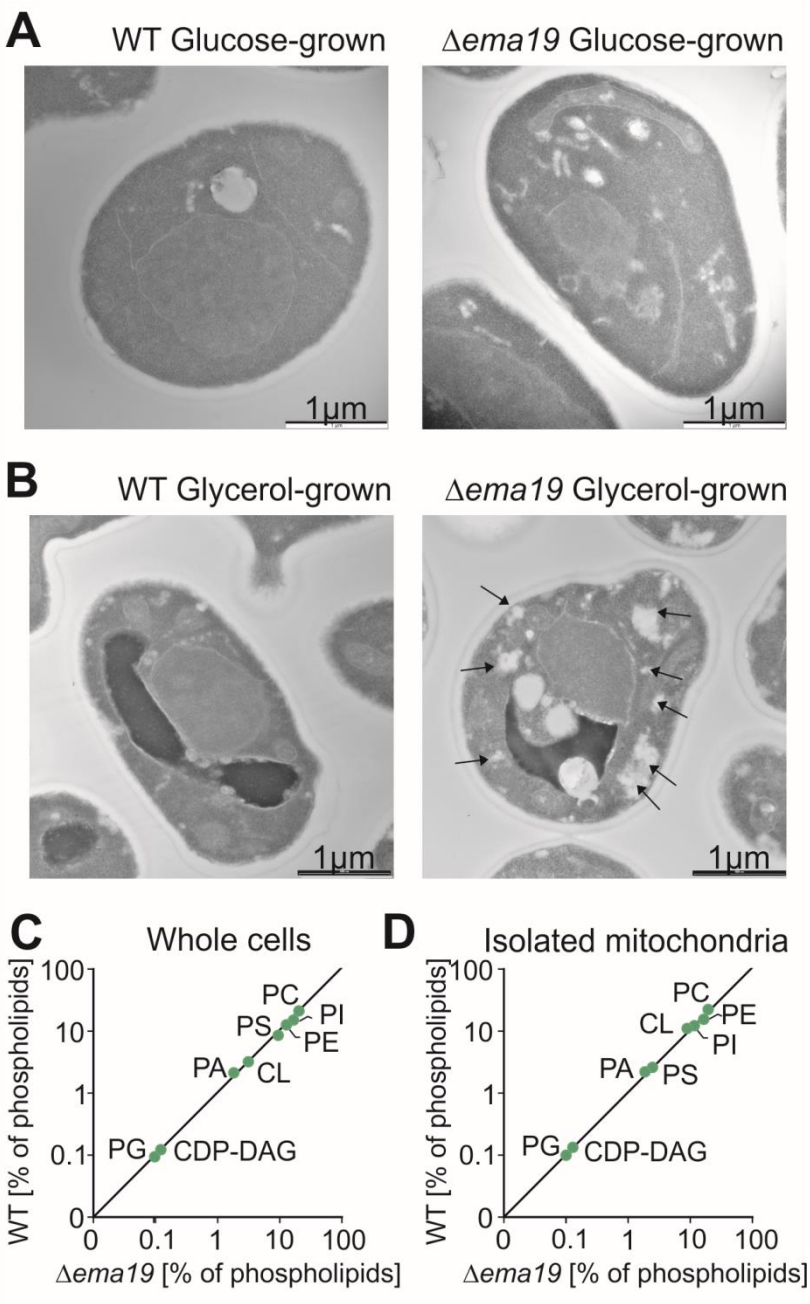

Figure 3. *Δema19* cells show morphological changes upon growth on glycerol. A, B. Yeast cells were grown to log-phase in media containing glucose or glycerol as carbon source. Cells were fixed in 2% glutaraldehyde, 3% formaldehyde over night at 4°C and treated as described (Prescianotto-Baschong and Riezman, 2002). Sections were analyzed by transmission electron microscope. Arrows point at the morphological structures observed in *Δema19* cells. More examples and enlarged images are shown in Fig. S4. **C, D.** The content of lipids in whole cell or mitochondrial extracts was analyzed by mass spectrometry and is shown here as % of total lipid mass. CDP-DAG, cytidine diphosphate diacylglycerol; CL, cardiolipin; PA, phosphatidic acid, PC, phosphatidylcholine; PE, phosphatidylethanolamine; PG, phosphatidylglycerol; PI, phosphatidylinositol; PS, phosphatidylserine.

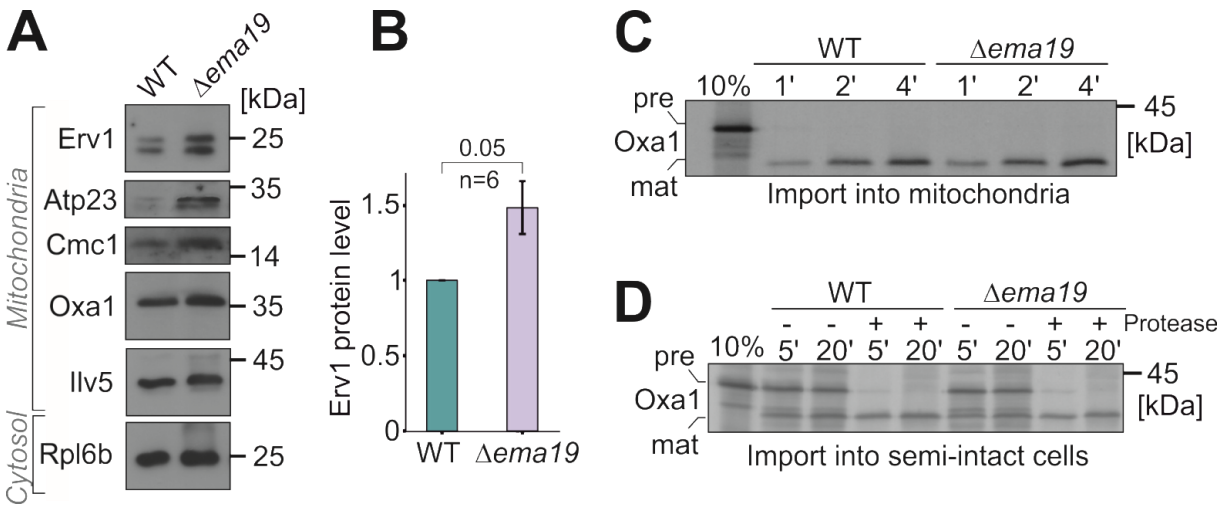

Figure 4. *Δema19* cells show increased levels of Erv1. A, B. The levels of the indicated proteins in whole cell extracts were analyzed by Western blotting. **C, D.** Radiolabeled Oxa1 was incubated with isolated mitochondria or semi-intact cells for the times indicated. Samples were treated with protease and analyzed by SDS-PAGE and autoradiography. pre, precursor; m, mature.

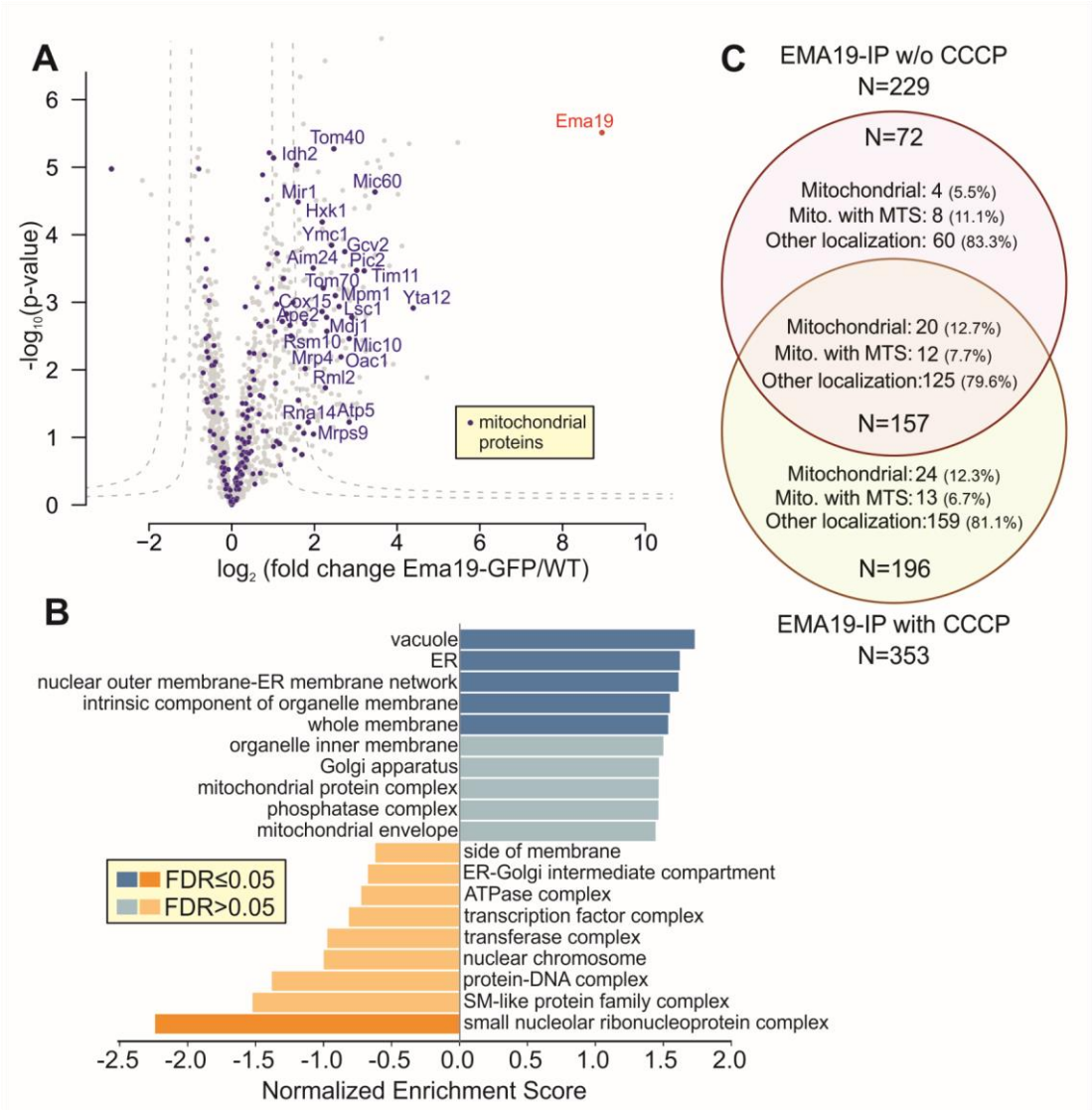

Figure 5. Ema19 interacts with many membrane proteins of the ER, of the vacuole and of mitochondria. A. Ema19-GFP and wild type cells were grown on glucose medium to mid-log phase, harvested and washed. Cells were lysed with glass bead lysis using NP40 as mild detergent. Extracts were cleared by centrifugation and incubated with GFP-Trap beads before bound proteins were analyzed by mass spectrometry. Data are based on four biological replicates for each strain. Enriched proteins are found in the upper right corner of the graph. Significant enrichment was tested with a two-sided T-test with permutation-based FDR cut-off to correct for multiple testing (S0=4, FDR<0.05 or FDR<0.01). **B.** Ema19-GFP interactors were analyzed using the WEB-based GEne SeT AnaLysis Toolkit algorithm (Liao *et al.*, 2019) and gene ontology groups are shown which are frequently found with Ema19 (in blue) or which are underrepresented (in orange). **C.** The mitochondrial membrane potential influences Ema19 interactions. Cells were treated for 1 h with the uncoupler CCCP to dissipate the mitochondrial membrane potential before cells were harvested and lysed with NP40. Ema19-GFP was isolated and interactors were determined by mass spectrometry. The full data set is shown in Table S5. Venn diagram showing proteins that were significantly enriched in the Ema19-GFP pull-down under the different conditions (S0=4, FDR<0.05). Mitochondrial localization according to Morgenstern *et al.* (Morgenstern *et al.*, 2017); MTS, mitochondrial targeting sequence.

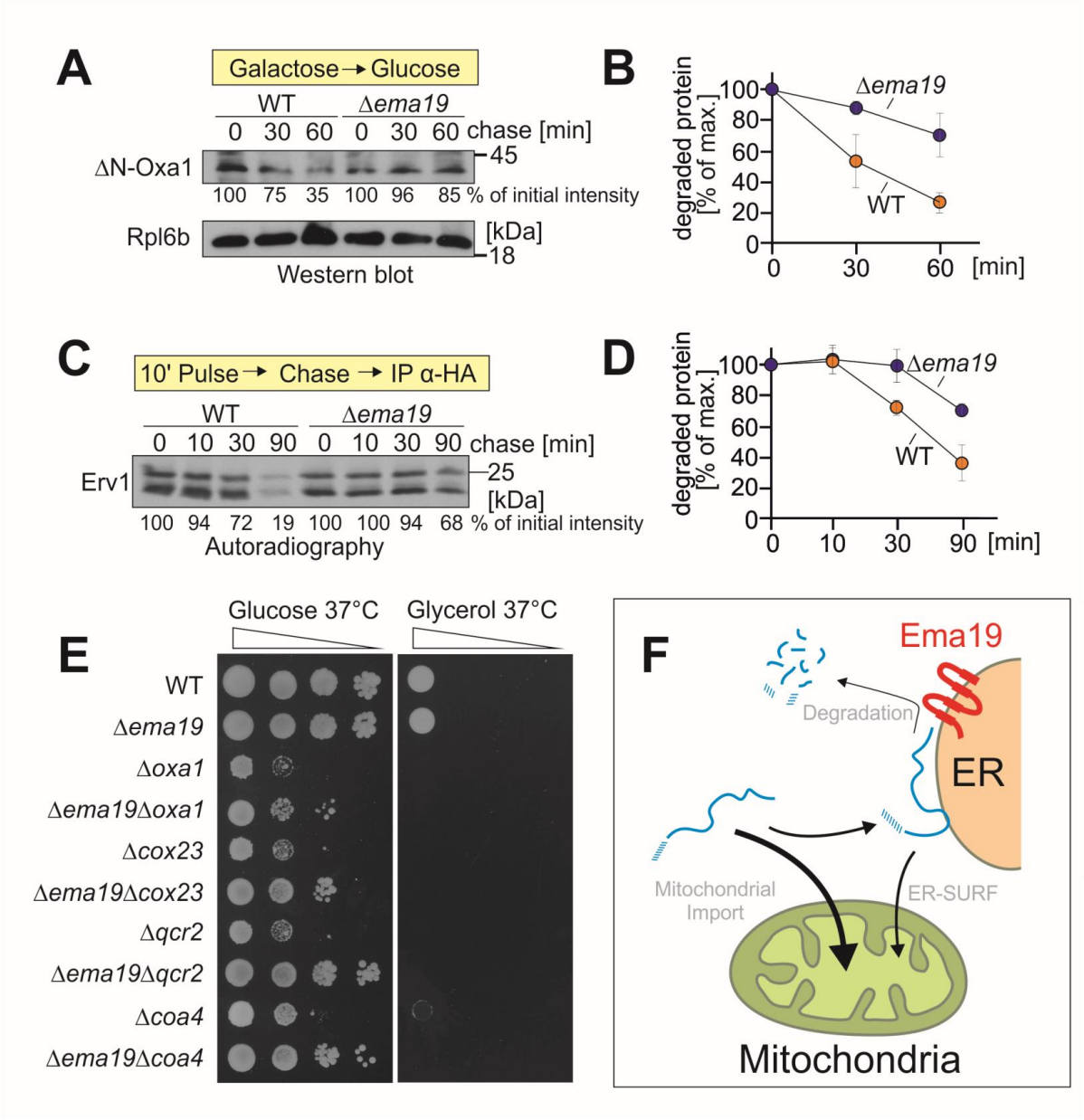

Figure 6. *Δema19* cells show reduced protein degradation. A. The non-importable ΔN-Oxa1 was expressed in wild type and *Δema19* cells. Expression was stopped by shifting cells from galactose to glucose for the times indicated (chase). Cells were isolated and the levels of ΔN-Oxa1 were analyzed by Western blotting and quantified. The ribosomal protein Rpl6b served as loading control. **B.** The results from three biological replicates were quantified. Mean and standard deviations are shown. **C.** Cells expressing HA-tagged Erv1 were grown to log phase. Radiolabeled methionine was added for 10 min (pulse). Cells were incubated in the presence of non-radioactive methionine (chase) for the times indicated. Cells were isolated, lysed and used for immunoprecipitation with HA-specific antibodies (IP α-HA). The levels of the radiolabeled Erv1-HA protein were detected by autoradiography. **D.** The results from three biological replicates were quantified. Mean and standard deviations are shown. **E.** Cells of the indicated strains were grown on galactose and dropped onto glucose- or glycerol-containing plates. **F.** Model for the role of Ema19 in the degradation of ER-associated mitochondrial precursor proteins.